Assessing Videogrammetry for Static Aeroelastic Testing of a Wind-Tunnel Model

Charles V. Spain[*], Jennifer Heeg[†], Thomas G. Ivanco[‡], Danny A. Barrows[§], James R. Florance[**], Alpheus W. Burner[††], Joshua DeMoss[‡‡]
NASA Langley Research Center, Hampton, VA 23681

Peter S. Lively[§§]
Lockheed Martin Space Operations, Hampton, VA 23681

The Videogrammetric Model Deformation (VMD) technique, developed at NASA Langley Research Center, was recently used to measure displacements and local surface angle changes on a static aeroelastic wind-tunnel model. The results were assessed for consistency, accuracy and usefulness. Vertical displacement measurements and surface angular deflections (derived from vertical displacements) taken at no-wind/no-load conditions were analyzed. For accuracy assessment, angular measurements were compared to those from a highly accurate accelerometer. Shewhart's Variables Control Charts were used in the assessment of consistency and uncertainty. Some bad data points were discovered, and it is shown that the measurement results at certain targets were more consistent than at other targets. Physical explanations for this lack of consistency have not been determined. However, overall the measurements were sufficiently accurate to be very useful in monitoring wind-tunnel model aeroelastic deformation and determining flexible stability and control derivatives. After a structural model component failed during a highly loaded condition, analysis of VMD data clearly indicated progressive structural deterioration as the wind-tunnel condition where failure occurred was approached. As a result, subsequent testing successfully incorporated near- real-time monitoring of VMD data in order to ensure structural integrity. The potential for higher levels of consistency and accuracy through the use of statistical quality control practices are discussed and recommended for future applications.

I. Introduction

A Videogrammetric Model Deformation (VMD) technique[1], developed at NASA Langley Research Center, was recently used to measure displacements and local surface angle changes on a static aeroelastic wind-tunnel model. The Variable Stiffness Spar (VSS) model[2] is part of a joint NASA, Air Force, and industry program known as the Active Aeroelastic Wing (AAW). The specific purpose of the VSS model was to demonstrate how a structural element governing the torsional stiffness and elastic axis position of the main wing box would allow modification of the static aeroelastic control surface effectiveness at different aerodynamic conditions. Testing of the VSS model was conducted in the NASA Langley Transonic Dynamics Tunnel (TDT)[3].

In the present VSS model work, VMD was used as a tool to measure main wing and control surface deflection angles that were used for several purposes, including the determination or validation of angle of attack, local incidence, control surface settings, aeroelastic deformation, leading edge divergence predictions, and control derivatives.

---

[*] Senior Research Engineer, Aeroelasticity Branch
[†] Senior Research Engineer, Aeroelasticity Branch, Senior Member AIAA
[‡] Aerospace Engineer, Aeroelasticity Branch
[§] Electronics Engineer, Advanced Sensing and Optical Measurement Branch, Member AIAA
[**] Aerospace Engineer, Aeroelasticity Branch, Senior Member AIAA
[††] Senior Research Scientist, Advanced Sensing and Optical Measurement Branch, Associate Fellow AIAA
[‡‡] Student, Virginia Polytechnic Institute and State University
[§§] Senior Engineer

II. The NASA Langley Transonic Dynamics Tunnel (TDT)

The NASA Langley Transonic Dynamics Tunnel (TDT), shown in figure 1, is a closed-circuit, continuous-flow, single-return wind tunnel. The test section is 16-feet square with cropped corners. It is capable of testing over a range of stagnation pressures from near zero to atmospheric and Mach numbers from near zero to 1.2, using either an air or an R-134a test medium. In the event of a model instability, the TDT also has the capability to reduce wind speed rapidly through the activation of four bypass valves that connect the test section area to the opposite leg of the wind-tunnel circuit. Designed specifically for aeroelastic testing, the TDT has been used for decades to conduct numerous aircraft, rotorcraft, and space-related aeroelastic and aeroservoelastic tests.

Figure 1. The NASA Langley Transonic Dynamics Tunnel (TDT).

III. Model Description

Figure 2 shows the VSS wind-tunnel model mounted in the TDT. The semi-span model was based on F/A-18A geometry and consisted of the right half of the vehicle. A remotely actuated spar beam, which was more flexible in the horizontal rather than vertical position, was located within the wing to affect the overall wing stiffness in both bending and torsion. Although not important for the purpose of this paper, reference 2 provides a more detailed description of the variable stiffness mechanism.

The wing had four control surfaces referred to as inboard leading edge (ILE), outboard leading edge (OLE), inboard trailing edge (ITE), and outboard trailing edge (OTE). The control surfaces were set manually between runs and locked into position. The deflection angles were originally set using a Model LCI-145-90 Jewell inclinometer with a verified accuracy of +/- 0.003 degree. The model pitch angle was set by a turntable controlled from the control room. During wind-on testing, Angle of Attack (AOA) becomes synonymous with the model pitch angle. AOA (and/or model pitch angle) was measured by an Allied Signal Model 700 Q-Flex accelerometer mounted in the center portion of the fuselage, which had a verified accuracy of +/- 0.001 degree.

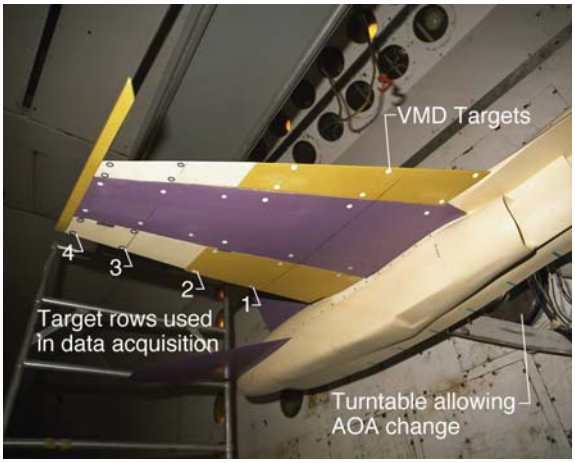

Figure 2. Photo of VSS model mounted in the TDT showing the VMD targets.

IV. Test Description and Events

The specific objective of the tests was to determine flexible static control derivatives of the model for a range of Mach Numbers and dynamic pressures (q). More specifically, changes in lift, pitching moment and rolling moment with respect to changes in AOA, and deflections of the four wing control surfaces were measured. This was accomplished by testing the model at low and high dynamic pressures with AOA- and control-surface-deflection variations in the range of approximately +/- 3 degrees. The model was loaded within safe limits as determined by pre-test analysis and laboratory testing.

There were two TDT test entries. The first was a four-week entry in October 2002, and the second was a one-week entry in January 2003. These tests are described in a separate paper[2]. In the first series of test runs, the test matrix consisted of three passes through the desired Mach number range at progressively higher stagnation pressures

(and thus densities), hence higher dynamic pressures. Early in testing there was a structural failure and loss of the ILE control surface. The failed surface was reconstructed, and after delay of about a week, testing resumed. The reconstructed ILE was fixed in place, so determination of derivatives for that surface was no longer possible. The test continued with the intent to determine derivatives with respect to the remaining three control surfaces, as well as with respect to AOA. Due to the loss of time associated with the ILE failure, testing was not completed during the October 2002 entry. However, a vacancy in the TDT in January 2003 allowed VSS model testing to continue.

Following the failure incident, the maximum q was slightly reduced and the number of Mach number passes was reduced from three to two. These passes were repeated several times with different combinations of fixed control surface deflection angles. Figure 3 shows the Mach and q conditions prior to the ILE control surface failure and after the ILE surface reconstruction on the first entry. On the second entry, the bleeds were accomplished at Mach 0.9 instead of Mach 0.85, but the q line passes were the same as indicated for post failure during the first entry.

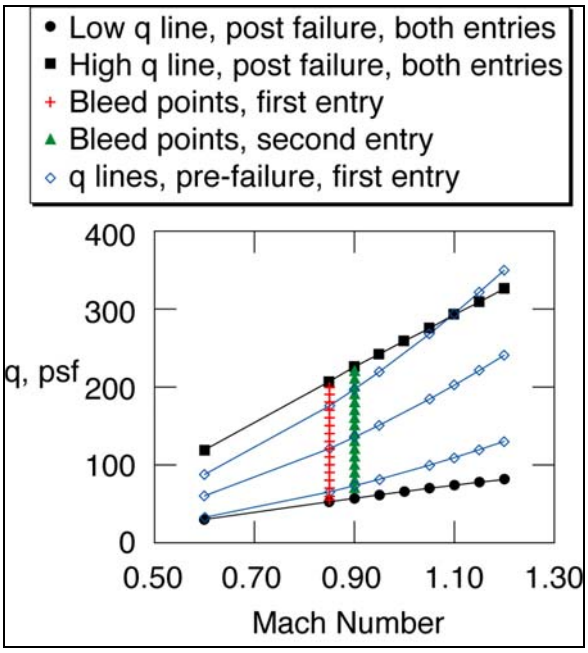

Figure 3: Tunnel test conditions before and after failure of the inboard leading edge (ILE) control surface.

V. VMD Description and Setup

The VMD measurement technique is an optical method characterized by automated image processing, sub-pixel resolution, near-real-time measurements, and high data volume with minimum impact to wind-tunnel test productivity. The technique consists of a single-camera, single-view, photogrammetric solution from digital images of targets placed on a wing or control surface with one coordinate known. Except for the targets, the technique is non-intrusive. The technique is described in detail in references 1, 4 and 5.

Graves and Burner describe the VMD measurement system used for the present tests in reference 6. This system is an upgrade of earlier VMD systems developed at NASA Langley. The upgrade includes an improved user and tunnel Data Acquisition System interface and a faster processing capability, making the technique more amenable to near-real-time monitoring.

Figure 4 shows a photograph of the model being prepared for VMD calibration. See page 747 of reference 1 for a description of the calibration principles and processes.

In figures 2 and 5, the subset of wing VMD targets used in data acquisition is identified. The targets are arranged in pairs, so that local angular deflections can be determined. For example, targets 1 and 2 can be used to determine angular changes for the ITE flap along row 1, and targets 15 and 16 can be used to determine angular

Figure 4: Preparations for VMD calibration.

changes on the main wing along row 3. These targets range in diameter from 7/16 to 3/4 inch and are 0.004-inch thick (typical paper thickness). Regardless of the target diameter, the system locates and uses the target center. For our purposes, the targets are considered non-intrusive with respect to flow and loads. Raw deflection data acquired during testing included translation positions (x (flow) and z (vertical) directions) for each target. The y (span) position was taken as known (i.e. measured by hand) and used in the computation of x and z. Data were acquired at each test point at 60 samples per second for 1/3 second during the first entry and for 1 second during the second entry. Deflection translations and deflection angles presented in this paper were determined in post-test processing. However, near-real-time processing and monitoring were at times used during testing to ensure model structural integrity.

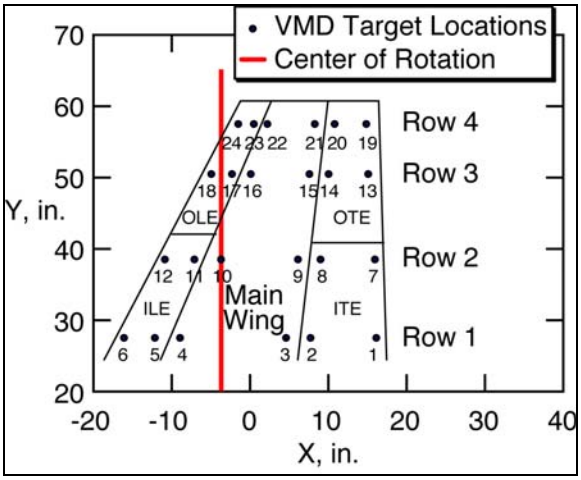

Figure 5. Planform locations of VMD targets and pitch angle rotation axis. Note that only the outer portion of the inboard control surfaces are shown.

VI. Assessment of VMD Accuracy and Consistency

A review of the uncertainty of the VMD technique itself for aerospace applications is found in reference 4. The present purpose is to assess the accuracy and consistency and demonstrate the usefulness of the system on a static aeroelastic test in the TDT. Although VMD measures two components (x-flow and z-vertical) of translation, the vertical displacements were of primary interest here. However, the measurements of undeformed x positions were also useful because along with z displacements, they allowed computation of local pitch angle changes of an imaginary line connecting two selected targets at a constant span station. Note that for this paper, the term "pitch angle" is used for wind-off measurements, and "angle-of-attack" is used for wind-on measurements, but the physical measurements are identical and both are referenced to the wind-tunnel centerline with leading edge up being positive in sign.

To assess the measurement consistency and accuracy without the complication of a flow field, the turntable was rotated through so-called Wind-Off-Zero (WOZ) polars. In the cases described here, the pitch angle was cycled from -2^o to $+2^o$ in 1^o increments. This process was repeated 13 times (typically before and after wind-on testing) throughout the second entry, and the resulting data was used to assess both the consistency and accuracy of the VMD system. For consistency, both displacement and angular measurements based on the 13 WOZ polars were used. The angular accuracy of the VMD measurements was assessed with comparisons to angular values determined by the onboard Q-flex AOA accelerometer. It should be noted that the assessment described herein was performed after the test had been completed and the equipment disassembled. For brevity, only selected samples of the data analysis based on the second entry are presented.

Because of the hysteresis and other nonlinearities of the model, it made no sense to compare raw position measurements between wind-off test points, because following a loading cycle, the model most likely would not return to the same zero-load shape as in another wind-off test point. Therefore, two comparisons were made: 1) the changes in vertical position with respect to change in pitch angle (slope of the pitch angle vs. vertical displacement curves) were compared for the 13 WOZ polars; and 2) angular displacements of the target pairs were compared with pitch angle changes indicated by the AOA Q-flex accelerometer. Because one of the main purposes of using VMD for static aeroelastic testing was to experimentally determine AOA and flexible control surface derivatives, the derived angular data were especially important.

A. Shewhart's Variables Control Charts

Consistency of the VMD system was evaluated using Shewhart's Variables Control Charts (also known as Statistical Quality Control (SQC) Charts). The e-Handbook of Statistical Methods[7] (sections 6.3.2.1and 6.3.2.2) is a handy online reference that describes the SQC methods used in the present work. Two types of charts were used in this study. When there are a small number of repeated measurements (samples) taken at about the same time and then repeated a number of times, then so-called $\overline{X}$ and R Control Charts for grouped data are appropriate. As an example, angular measurements were determined for several target pairs during a single test point, and this process was repeated for each of the 13 WOZ polars. $\overline{X}$ is the group measurement average (several average angular

deflections determined from measurements at a single test condition), and *R* (range) would be the $X_{maximum}$ minus $X_{minimum}$ for each group. These values are determined for all groups (in this case 13), and Upper and Lower Control Limits (UCL and LCL, which are based on statistical 3σ limits) are determined for both $\overline{X}$ and *R*. If all the individual terms fall within the control limits, then future measurements would be expected to follow suit. Statistical control is achieved when all samples are within limits (group averages within $\overline{X}$ control limits and dispersion of individual samples in a group within *R* control limits). A violation of the limits should be rare (probability about 0.3% for a normal distribution[7]) and would justify an investigation to determine if the system has changed or become unstable.

The Individuals Control Charts (also known as X (individual values) and MR (moving range) charts) were also used for analysis. In the case where only a single sample, of value *X*, is determined at a time and repeated a number of times, Individuals Control Charts are appropriate. As an example, a single target deflection at a selected pitch angle was measured and then repeated for 13 WOZ polars. For Individuals Control Charts, the average ($\overline{X}$) is determined by all samples (13 in this case), and *MR* is determined by the absolute difference between each two consecutive data points ($|x_1-x_2|$, $|x_2-x_3|$…$|x_{12}-x_{13}|$). Pairs of consecutive data points can therefore be referred to as pseudo groups of 2. The control limits are then determined in the same manner as for $\overline{X}$ and *R* Charts, except that the statistical factors are based on 2 samples per pseudo group. The system is deemed within statistical control if individual samples fall within limits on the *X* chart and the maximum absolute differences between sample pairs fall within the *MR* limits. Although it may have been wiser to have taken multiple points at each condition so that the $\overline{X}$ and *R* Charts could be used, in the interest of meeting many test objectives with limited tunnel time, this was not done.

B. Statistical Quality Control Assessment

Recall that figure 5 presents the numbering of the individual targets. Local pitch angle changes are determined by the measured change in vertical position of an upstream target with respect to the downstream target of a target pair, dividing by the distance between the two targets (also measured with VMD), and converting radians to degrees. For the data presented here, leading-edge-up is considered positive for all 12 target pairs. In this way, the local angular changes can be easily compared to changes in model pitch angle.

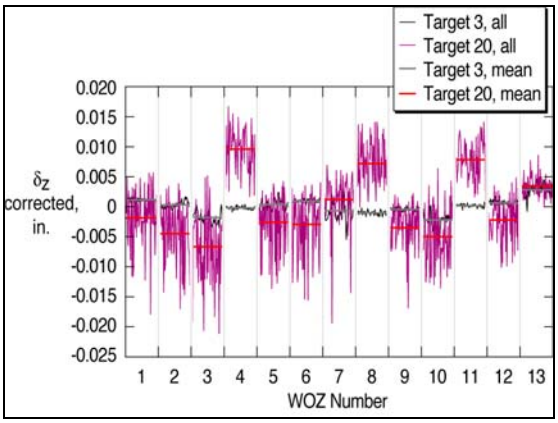

Figure 6: Examples of variation in 60 samples-per-second data, model pitch angle = +2°.

During the second entry, VMD data were acquired at 60 samples per second for one second during each test point. For the SQC assessment, only the mean data were used. However, the individual sampling is of interest. Figure 6 shows all of the 60 samples-per-second data acquired during the 13 WOZ polars for targets 3 and 20 along with the mean data for each 1-second sampling. These data were acquired at model pitch angle of 2°, and were corrected by subtracting out the mean value from all 780 samples (13 WOZs x 60 samples per WOZ polar). The plots indicate that the individual samples vary much more from the mean for target 20 than for target 3, and that even the 1-second mean data show much greater variation for target 20 than for target 3. It can be observed that the 1-second means for target 20 may vary from the overall mean by about 0.01 inch, whereas target 3 means vary by only about 0.003 inch.

Target 20 is on the OTE control surface and target 3 is on the main wing inboard. A similar view of 60 samples-per-second data for all 24 targets (not shown) indicates that the variations for the 8 outboard control surface targets were similarly greater than those on the entire main wing as well as those on the inboard control surfaces. This issue will be further discussed.

Figure 7 shows examples of measuring the target displacement slopes with respect to changes in model pitch angle for VMD target 24. In the figure for WOZ 8, the 5 points taken in the polar are used in a linear regression to determine the slope. The slopes and intercepts of all the targets were determined this way. However, note that for WOZ 7, the point at model pitch angle of -2° does not align with the other 4 points as it should for simple near-rigid rotation of the wing on the turntable. Such an anomaly is much greater in magnitude than the inconsistencies generally observed in the test data. In total, there were 34 out of 1560 WOZ target point measurements which were obviously bad. All of the bad points were at model pitch angle of -2° and occurred at targets 20 through 24, which

are all on row 4 near the wing tip. Target 19, also on the tip row, was not so affected. This is of obvious concern, mainly because it is not known how many bad points are in the wind-on data. This will also be discussed later.

In order to show variance in the measurements, trend-line equations (slopes and intercepts) were used to compute the z that was subtracted from the measured raw z position of the target. This indicates departure from linearity of the individual measurements. Figure 8 shows the range (maximumum-minimum) of these nonlinearities at the targets on rows 1 and 3. Here we see that the nonlinearities for targets on the outboard control surfaces (targets 13, 14, 17 and 18) tend to be greater than the others. By referring to figure 5, it can also be concluded that the difference in behavior on the outboard control surfaces is not due to distance from the rotation center.

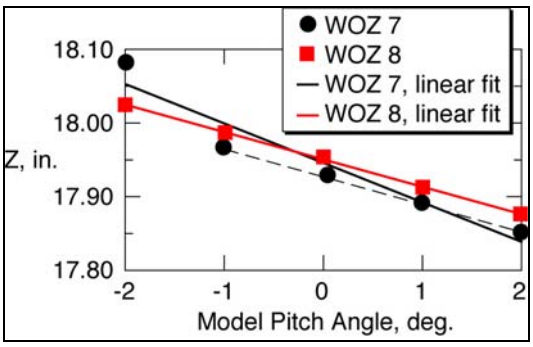

Figure 7: Regression analysis revealing bad data point for target 24 measurements. Bad data point occurs for WOZ 7 at -2° model pitch angle.

Figure 9 shows Individuals Control Charts for the slope variation of target 17, which as seen on figure 8, has the greatest nonlinearities of the 12 targets shown. In the X chart, the difference between the X limits (UCL and LCL) and the average ($\overline{X}$) is about 0.003 inches/degree, which despite the issues described, is encouraging in terms of consistency. The MR chart indicates that the maximum dispersion between points within the pseudo groups would be about 0.0036 inches/degree.

Because of the importance of the angular measurements described above, because rows 1 and 3 were along the center of the control surfaces (the most desirable location to determine control surface angles, see figure 2), and finally because of the problem targets on row 4, the remaining SQC description will be based on rows 1 and 3 and the derived angular deflections. The raw data used in determining the angular deflections of the 6 target pairs on rows 1 and 3 were all acquired simultaneously at each test point. Once the raw angles were computed, they were first corrected by subtracting out the target pair angle at 0° pitch angle and then scaled to the exact nominal pitch angle (-2, -1,1, and 2°). Therefore, the resulting six grouped angular displacements should all agree with the similarly scaled model pitch angle measurement from the Q-flex accelerometer. In figure 10, the R chart shows that the dispersion within groups should be within 0.15°, and the group averages ($\overline{X}$) should be within about +/- 0.04° of the grand average ($\overline{\overline{X}}$). In addition to consistency, these charts also indicate accuracy when compared to the corrected angle of exactly -2° measured by the Q-flex accelerometer.

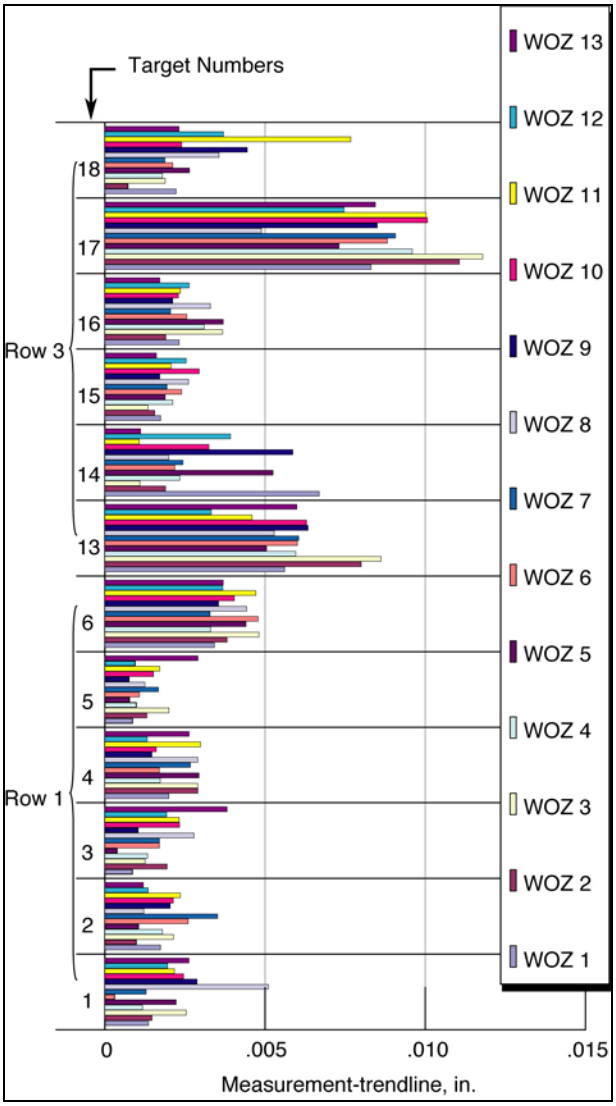

Figure 8: Nonlinearities in measurements of target displacements.

Figure 10 groups all six measurements together and is an indication of overall performance of the VMD system. However, it was observed that some targets displayed different behavior from others; therefore, the assessment was repeated using Individuals Control Charts. For these charts, each of the 6 target pairs was evaluated individually for the 13 WOZ polars. Figure 11

contrasts one of the most consistent pairs (targets 15 and 16 on the main wing) with one of the least consistent (targets 17 and 18 on the OLE). These data correspond to a model pitch angle of +1°. For the outboard leading edge, angular measurements can be expected to be consistently within +/-.08° from the measurement average. For accuracy in comparison to the Q-flex accelerometer measurement, a sample near the lower control limit would be in error by about 0.15°. The outboard leading edge is the worst case for all of the angular measurements on rows 1 and 3. Obviously, the measurements of the main wing on row 3 (shown in red) are much more consistent and accurate. The table summarizes the consistency and accuracy for all six target pairs.

A major objective of the wind-tunnel tests was to determine flexible control surface and AOA derivatives. It was therefore important to be able to measure control surface deflection angles as accurately as possible. Values in the table identified with an * are the worst-case conditions used to ascertain the derivative uncertainties. Worst-case uncertainty estimates for the lift derivatives for AOA and the three moveable control surfaces (ITE OLE and OTE) are +/- 2.6%, 3.2%, 7.2%, and 4.5% respectively.

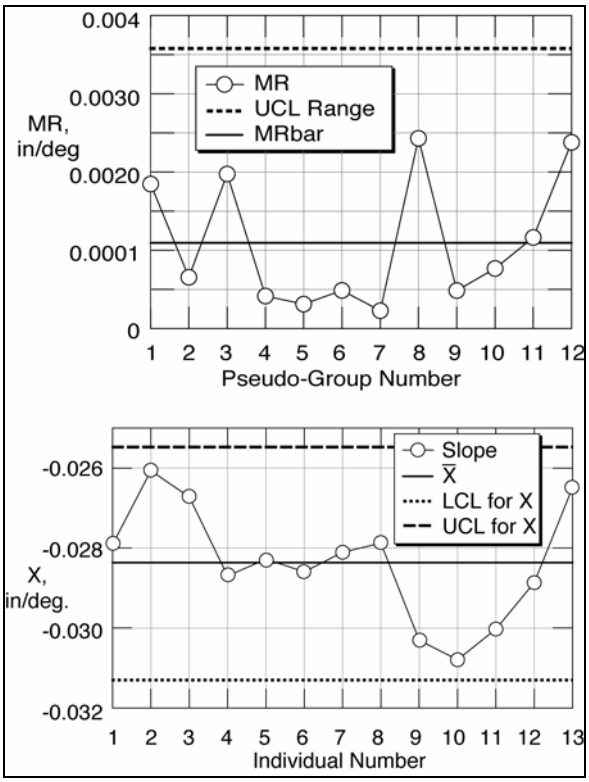

Figure 9: Individuals Control Charts for target 17 slopes.

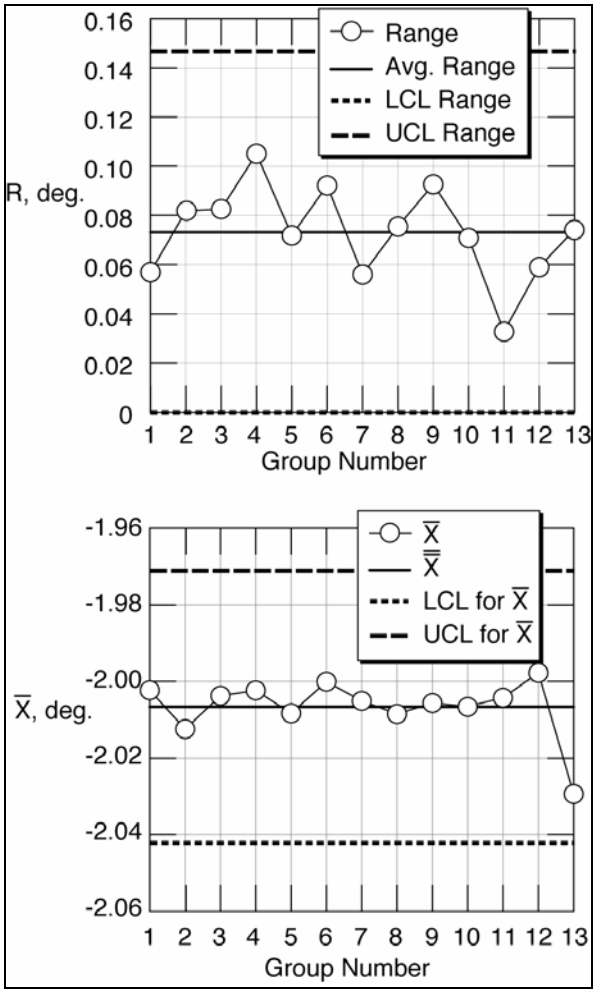

Figure 10: $\overline{X}$ and R charts for grouped surface angles.

The post-test consistency and accuracy assessment identified several issues that will be discussed briefly. First, bad data points were discovered that, at present, are unexplained, and similar bad points could have occurred during wind-on testing. As previously described, there was more variability in the VMD measured data on the outboard control surfaces than at other locations, even though there was no wind or other significant structural excitation during the wind-off testing. Possible explanations are a) the wing was gradually changing shape (creeping, settling) as internal stresses from previous loadings were relieved; b) low level building and turntable vibration produced vibration on the control surfaces or VMD camera; c) electrical noise; and d) glare, contrast or angular orientation interfered optically with certain targets. These possibilities have recently been explored with no definitive resolution. It is conceivable that these mysteries could have been cleared up if the data had been more thoroughly analyzed with the test apparatus still in place.

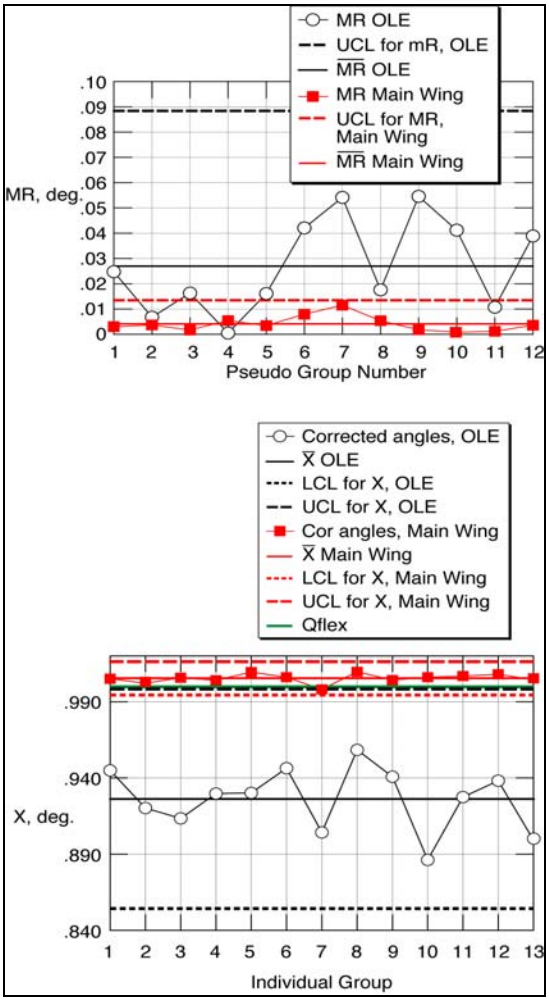

Figure 11: Contrast in Individuals Control Charts between two target pairs, OLE row 3 and main wing row 3, at model pitch angle = +1°.

Table - Summary of VMD Angle Assessment

	Surface (target pair in row number)						
	ILE (row 1)	Main wing (row 1)	ITE (row 1)	OLE (row 3)	Main wing (row 3)	OTE (row 3)	Angle Q-flex
$\overline{X}$ deg.	-1.975	-2.007	-2.000	-2.042	-2.005	-2.010	-2.0
	-0.993	-1.005	-1.001	-1.092	-1.004	-1.009	-1.0
	1.008	0.991	1.005	0.926	1.005	0.996	1.0
	2.040	1.996	2.000	1.931	2.011	2.011	2.0
$\frac{\delta \overline{X}_{CL}}{2}$ degree	0.065	0.007	0.025	0.042	0.015	0.036	-2.0
	0.058	0.020	0.019	0.041	0.012	0.045*	-1.0
	0.040	0.026*	0.032*	0.072*	0.011	0.038	1.0
	0.053	0.025	0.024	0.039	0.012	0.030	2.0
UCL for *MR* degree	0.079	0.022	0.031	0.052	0.019	0.044	-2.0
	0.071	0.025	0.023	0.050	0.015	0.055	-1.0
	0.049	0.032	0.039	0.088	0.013	0.047	1.0
	0.065	0.031	0.030	0.048	0.015	0.037	2.0
Error, degree	0.025	-0.007	0.000	-0.042	-0.005	-0.010	-2.0
	0.007	-0.005	-0.001	-0.092	-0.004	-0.009	-1.0
	0.008	-0.009	0.005	-0.074	0.005	-0.004	1.0
	0.040	-0.004	0.000	-0.069	0.011	0.011	2.0

Where $\overline{X}$ *is corrected angle average for 13 WOZs,* $\frac{\delta \overline{X}_{CL}}{2}$ *is the distance from average to control limits,* UCL for MR *is upper control limit for moving range, error is difference in corrected average angle and corrected Q-flex reading, and * identifies the worst-case conditions used for derivative uncertainties.*

Nevertheless, the VMD system as implemented on these tests provided reasonably accurate data in most cases. The data analysis on many of the targets, especially those not on the control surfaces, indicates that the system is capable of a higher level of precision than achieved in these tests. Process improvements and investigation of unexplained phenomena may prove beneficial in the future.

VII. Leading Edge Control Surface Departure Incident

During the first entry, just after a test point at the highest Mach number and q, the ILE control surface suddenly deformed (leading edge up) and departed from the model. In the aftermath of the incident, the failure was investigated, and a replacement ILE control surface was constructed.

The VMD data, examined after the incident, revealed that the ILE control surface probably started deteriorating during run 17 and continued through run 18. This deterioration is indicated in figure 12 which shows the relative aeroelastic deflection of the ILE control surface. The relative aeroelastic deflection angle is defined here as the deformed angle of the control surface with respect to the deformed angle of the main wing on the same row (recall figure 5). Testing prior to the ILE failure was conducted at the low, middle, and high q conditions as described earlier. The data in figure 12 represents a consistent AOA of +1°, with the VSS in the horizontal (more flexible) position. Observe that at the highest Mach number for the high q condition prior to failure, there is a sudden change in aeroelastic deflection of the ILE control surface. Subsequent test points (shown in red) all show relatively higher aeroelastic deformation, indicating that the structure had changed. At high q, the degradation is even more dramatic, and the ILE control surface departed the model just after the high q point at Mach 1.2.

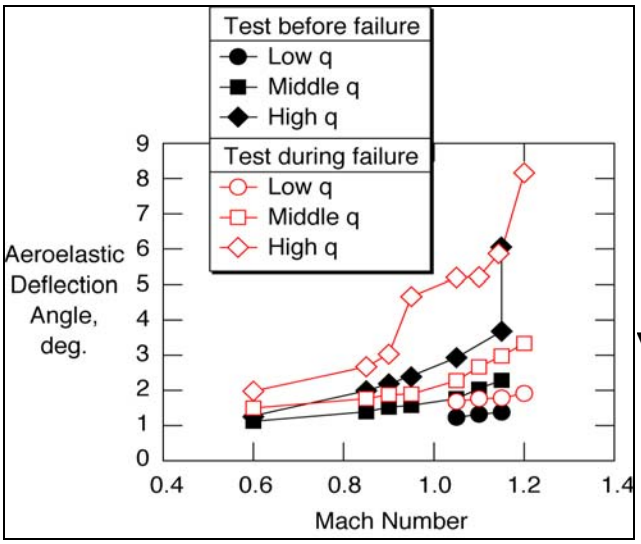

Figure 12: Relative aeroelastic deformation of the ILE control surface leading to failure, AOA = +1°.

Unfortunately, the test team was not monitoring aeroelastic angular deflections in real time during these runs. The model, based on pretest analysis and test loading, was not expected to fail. As it turned out, a faulty bond in the ILE control surface composite skin was the most likely cause of the incident. However, after learning the hard way, the test team developed a near-real-time monitoring system that was used for the remainder of the VSS testing.

VIII. Near-Real-Time Deflection Monitoring of Mean Data

Following the incident, in the interest of model safety, a near-real-time method was adopted in order to monitor aeroelastic deformation. At each test point, total aeroelastic deformations of the mid section of target rows were checked, along with relative aeroelastic deflection of the control surface target pairs, before proceeding on to higher Mach and q conditions.

Figure 13 shows typical relative aeroelastic deflections monitored during the remaining VSS testing. These data represent the low and high q runs and flow density increases (bleeds) at constant Mach Number during the second entry (recall figure 3). The control surface positions were set to zero for these runs, and AOA polars were included. It can be observed that the relative aeroelastic deformations did not approach the magnitudes shown just prior to the incident (see figure 12). The behavior represented in this figure was typical of the data monitored in near-real time for the remainder of the test. No further structural degradation was observed.

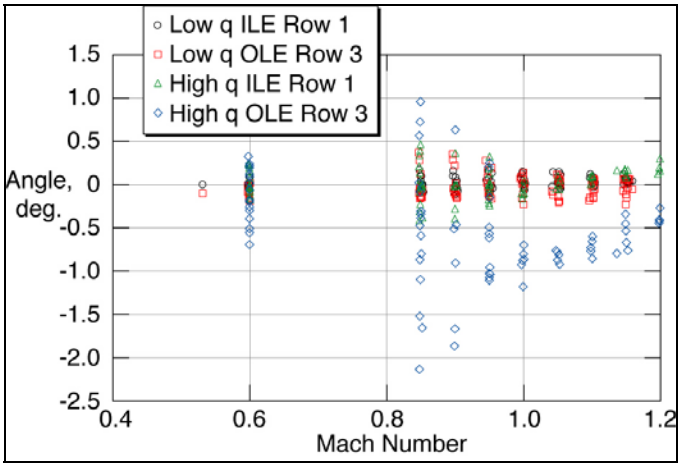

Figure 13. Relative aeroelastic deformation of both leading edge control surfaces for the second entry, runs 5 and 6.

IX. Lessons Learned

The assessment of VMD accuracy and consistency identified both good and bad aspects of the measurement system as implemented. Unexplained phenomena, such as bad data points on the tip row at -2° model pitch angle and the difference in consistencies when comparing the outboard control surface target measurements with measurements at the other targets (both 60-samples-per-second data and the 60- samples-per-second means) indicate the need for further investigation. On the other hand, the VMD measurements were generally very precise. Users would benefit most from use of the VMD system if an ongoing statistical quality control effort were established in which discrepancies were investigated and performance was tracked, documented, and updated with every use. The VMD system should be extensively exercised prior to and during actual wind-tunnel tests, including processing and evaluating both the results and quality in near-real time. This way, problems identified can be investigated while the test apparatus is in place and before critical data acquisition is completed. Multiple data points should also be acquired at each test condition so the statistical base will be as rich as possible.

The procedures suggested above would lend a higher level of confidence to the VMD applications described in this paper (such as measuring surface angles for determining flexible stability and control derivatives and monitoring structural integrity). It would also encourage other uses, such as static aeroelastic divergence prediction,

validation of aeroelastic trim analysis, and even recordings of operational dynamic or flutter mode shapes (using high sampling rates).

Finally, it was learned that when properly employed, near-real-time monitoring of VMD data can be effective in avoiding structural failure of aeroelastic wind-tunnel models.

X. Summary and Conclusions

For the VSS wind-tunnel tests, accurate measurement of aeroelastic deformation was critical to success. The use of a Videogrammetric Model Deformation (VMD) system in these static aeroelastic wind-tunnel tests was described along with a Statistical Quality Control (SQC) assessment of the data measurements and the results of some of the VMD-based measurements. The uses described included the determination of flexible static stability and control derivatives and the evaluation of structural integrity during and after wind-tunnel loading. The SQC assessment identified some specific consistency and accuracy issues in need of investigation.

VMD was shown to be invaluable in the post-incident assessment of a control surface degradation and failure. Based on that experience, near-real-time monitoring of the aeroelastic deformation via VMD was adopted in order to avoid any additional structural failures.

VMD has proven to be an accurate and practical method of determining point displacements as well as local angular deflections. It is ideally suited for laboratory or wind-tunnel testing. The VSS test team found VMD especially suitable for static-aeroelastic testing. However, the benefits of the VMD system were not fully realized in the VSS tests, so with the hopes of improving future VMD use, suggestions were made to include the use of statistical quality control practices during testing.

References

[1]A. W. Burner, and Tianshu Liu, "Videogrammetric Model Deformation Measurement Technique," *Journal of Aircraft*, Vol. 38, No. 4, pp. 745-754, July-August, 2001.

[2]James R. Florance, Jennifer Heeg, Charles V. Spain, Thomas G. Ivanco, and Carol D. Wieseman, "Variable Stiffness Spar Wind-Tunnel Model Development and Testing," AIAA-2004-1588, April 2004.

[3]Stanley R. Cole, and Jose A. Rivera, Jr.: *The New Heavy Gas Testing Capability in the NASA Langley Transonic Dynamics Tunnel*. Paper No. 4, presented at the Royal Aeronautical Society Wind Tunnels and Wind Tunnel Test Techniques Forum, Churchhill College, Cambridge, UK, April 14-16, 1997.

[4]A.W. Burner, Tianshu Liu, and Richard DeLoach, "Uncertainty of Videogrammetric Techniques used for Aerodynamic Testing," 22nd AIAA Aerodynamic Measurement Technology and Ground Testing Conference, St. Louis, Missouri, AIAA 2002-2794, 20 pages, June 2002.

[5]Jennifer P. Florance, Alpheus W. Burner, Gary A. Fleming, Craig A. Hunter, and Sharon S. Graves, "Contributions of the NASA Langley Research Center to the DARPA/AFRL/NASA/Northrop Grumman Smart Wing Program," AIAA Dynamics Specialists Conference, Norfolk, VA, AIAA 2003-1961, April 9-10, 2003.

[6]S. S. Graves, and A. W. Burner, "Development of an Intelligent Videogrammetric Wind Tunnel Measurement System," Optical Diagnostics for Fluids, Solids, and Combustion, SPIE International Symposium on Optical Science and Technology, San Diego, CA, 29 July to 3 August, 2001.

[7]NIST/SEMATECH e-Handbook of Statistical Methods, http://www.itl.nist.gov/div898/handbook/, December 11, 2003.